THE UNIVERSITY OF MICHIGAN

COLLEGE OF ENGINEERING
Department of Electrical Engineering
Space Physics Research Laboratory

Scientific Report No. JS-6

ELECTRON TEMPERATURE EVIDENCE FOR NONTHERMAL EQUILIBRIUM IN THE IONOSPHERE

N. W. Spencer
L. H. Brace
G. R. Carignan

ORA Project 03599

under contract with:

NATIONAL AERONAUTICS AND SPACE ADMINISTRATION
CONTRACT NASw-139
WASHINGTON, D.C.

administered through:

OFFICE OF RESEARCH ADMINISTRATION ANN ARBOR

May 1962

Electron Temperature Evidence for Nonthermal Equilibrium in the Ionosphere

N. W. SPENCER,[1] L. H. BRACE, AND G. R. CARIGNAN

University of Michigan, Ann Arbor, Michigan

Abstract. A brief review of the theoretical and experimental aspects of the 'dumbbell' electrostatic probe experiment is given. The electron temperature and positive ion density data resulting from its use in two flights at Fort Churchill, Manitoba, Canada, in the spring and early summer of 1960, and in two flights at Wallops Island, Virginia, in midsummer 1960 and spring 1961, are presented and discussed. The electron temperature profiles exhibit large positive gradients between 150 and 250 km, gradually changing to an approximately isothermal region (approximately 2800°K) above 250 km. An exception to this was the second Wallops Island measurement in which a negative temperature gradient was observed above 250 km, in a quiet ionosphere. The ion density profiles show only slight density maxima in the E region, the less distinct F_1 regions, and, at Wallops Island, well defined F_2 maxima at about 300 kilometers. Electron density data from (1) two-frequency beacon experiments flown on the same rockets, and (2) simultaneously recorded ionograms are presented for comparison. It is noted that good agreement is obtained between the electron density measured by the two different techniques and the ion density as measured by the dumbbell technique. It is concluded, on the basis of additional temperature data obtained from a small cylindrical probe that the dumbbell experiment measures temperatures that are representative of all thermal electrons. It is further concluded that if gas temperatures derived from satellite drag measurements and other techniques are valid as generally accepted, electrons and neutral particles are not in thermal equilibrium in the daytime ionosphere to altitudes of at least 420 km. Finally, it is observed that the electron temperature varies significantly with the state of the ionosphere, electron temperatures being higher and more variable in the more disturbed ionospheres.

Introduction. The earth's ionosphere, the extensive region of the very high atmosphere composed of neutral and ionized particles, has been the subject of increasingly intensive study since its presence was first suggested some 80 years ago by Stewart, and postulated 20 years later by Heaviside and Kennelly. Until about 1925, when Appleton and Barnett measured arrival angles of reflected electromagnetic waves, and thus specifically demonstrated the existence of a region of charged particles, work was confined largely to theoretical studies. About this time, however, Breit and Tuve devised a scheme for transmitting short pulses of radio frequency energy vertically and for studying the reflected signal to obtain quantitative measurements. This 'ionosonde' technique has been developed extensively over the years and today provides a large amount of quantitative, world-wide data (ionograms), from which one may determine electron densities up to the level of the density maximum (~300 km).

The ionosonde method, although providing data that have made possible much of our present knowledge of the ionosphere, has two major drawbacks in that it is an indirect method and, for an earth-bound station, is limited to measurements below the F_2 maximum. Further, interpretation of ionograms is sometimes a difficult and controversial matter,[2] and, in some cases, e.g., a spread F condition, is not generally feasible.

As with most scientific studies of an experimental nature, one prefers to conduct as nearly direct measurements of the desired quantities as the technology and other aspects permit. In particular reference to the ionosphere, direct measurements became possible when the V-2 rocket was made available for performing scientific measurements. Passage of the rocket

[1] Now with the NASA-Goddard Space Flight Center.

[2] See, for example, Program of URSI Annual Meeting, Commission 3, Washington, D. C., 1961.

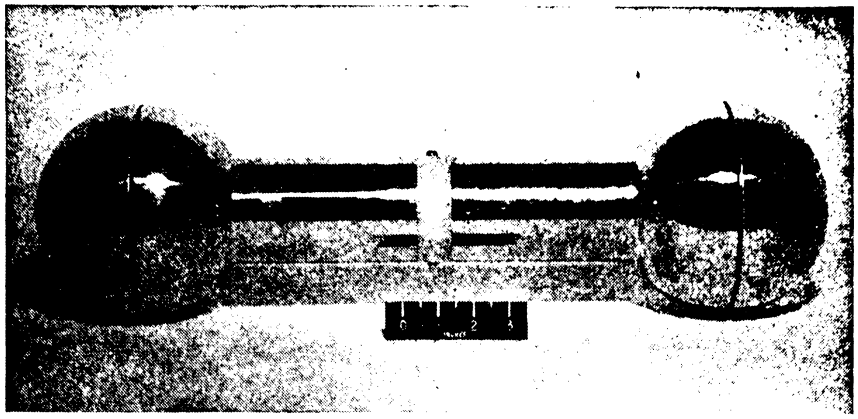

Fig. 1. The dumbbell electrostatic ionosphere probe.

through the lower ionosphere made possible two broad types of measurements: those resulting from (1) an analysis of the effects of charge on the passage of an electromagnetic wave as the rocket progressed through the region, and (2) techniques that measure strictly local properties, with the rocket as the reference point. Both types were undertaken initially; the former, however, not requiring a knowledge of the specific manner in which the rocket might alter its environment, and being more closely allied to the already existing ionosonde technique, received the greatest attention and has, over the years, been more extensively developed [*Seddon,* 1953; *Berning,* 1960]. Measurements employing these radio propagation techniques have yielded data in essential agreement with ground-based measurements, and the results have received orderly publication in appropriate technical journals [*Jackson, Kane, Seddon,* 1956; *Berning,* 1960].

The second general technique has not, until more recently, been at all adequately undertaken, although several exploratory Langmuir probe experiments to determine electron temperature were carried out using the V-2 rocket by University of Michigan experimenters. Another direct measurement technique adopted somewhat later uses the changing impedance of a dipole antenna with passage through the ionosphere to provide electron density measurements [*Jackson and Kane,* 1959].

The early experiments employing the Langmuir probe technique, or, more generally, the electrostatic probe technique, took the form of a rather simple electrode (truncated conical sleeve) mounted at the nose of the rocket. A relatively large magnitude sawtooth voltage (in terms of now well-known electron thermal energies) was applied between the electrode and the rocket, and the resulting current was telemetered to ground. Subsequent attempts at interpretation of the resulting data revealed the shortcomings of the exploratory instrument and stimulated extensive theoretical study which, on the basis of certain assumptions relative to rocket surface properties, probe geometry, electron energy distribution, ion mass, etc., indicated that good measurements of electron temperature and positive ion density should be realizable. These results are documented in early reports and papers, which were published in the literature [*Dow and Reifman,* 1949; *Hok, Spencer, and Dow,* 1953; *Hok, Spencer, Dow, and Reifman,* 1951].

Several years later, when the opportunity to carry on the experiment was again at hand, the results of the earlier work were used as a starting point. It was concluded that ejecting an appropriate probe instrument from a suitable rocket into the ionosphere offered the greatest likelihood of obtaining valid measurements. This approach eliminated the necessity of considering varying surface conditions, the effect of escaping gas, the presence of unwanted potentials, and other uncertainties necessarily encountered by using the rocket as one of the probe electrodes. Accordingly, a probe of simple geometry, appropriate to a straightforward theoretical treatment, and state-of-the-art instrumentation, was selected. Figure 1 illustrates the instrument that was developed and is being employed in the basic experiment reported herein. Several developmental experiments were carried out, with

varying degrees of success [*Boggess, Brace, and Spencer*, 1959].

The dumbell-shaped instrument electrically simulates two spherical electrodes isolated in the ionosphere connected by a suitable voltage generator and current indicating device. The dumbbell, in addition to functioning as an electrostatic probe, acts entirely independently as a dipole antenna for the internally contained telemeter.

Theory of the measurements. The theoretical basis for the experiment can be described in the following manner: Assume a spherical conductor immersed and at rest in the ionosphere where there exists thermal equilibrium, for each particle species at least, and a mean free path long with respect to the sphere diameter. In this case, the random current density of a particular species of charged particles some distance from the sphere can be represented by the expression

$$J = Ne\sqrt{\frac{kT}{2\pi m}} \tag{1}$$

where

J = random current density.
N = particle number density.
e = electron charge.
T = particle kinetic temperature.
m = particle mass.
k = Boltzmann constant.

Assuming that the predominant ion is O^+ [*Johnson, Meadows, Holmes*, 1958], the ratio of electron to ion current density is about 170 or the square root of the mass ratio of these two components. This is the ratio of the number of electrons to the number of positive ions (number density of negative ions is considered negligi-

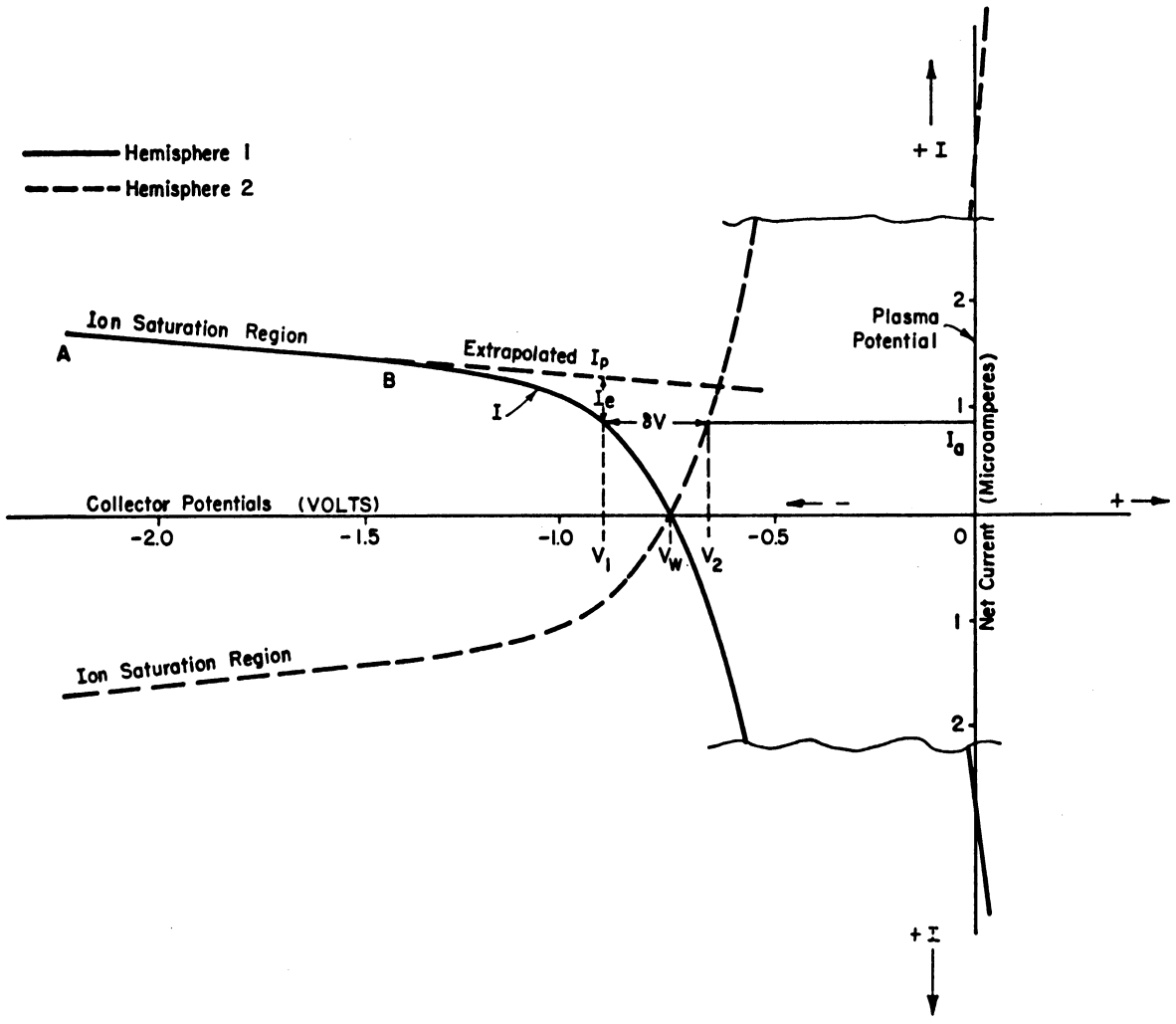

Fig. 2. Volt-ampere characteristics of the dumbbell probe hemispheres.

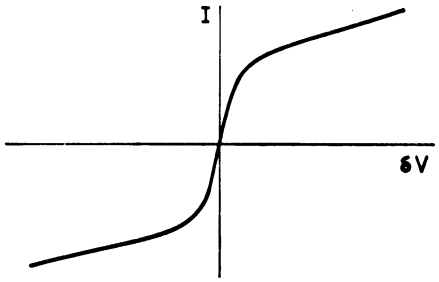

Fig. 3. A composite volt-ampere characteristic of the dumbbell probe.

ble) that would cross a unit area in unit time in the region. This will not, however, be the case at the surface of the sphere because the predominance of electron flux will charge the sphere negatively, thus accelerating ions and retarding electrons. Potential equilibrium will be established, when the electron and ion fluxes are equivalent, for a sphere potential defined in this paper as the wall potential, V_w.

The magnitude of the electron current that flows to the sphere under equilibrium is given by

$$I_e = A_e J_e \exp\left(\frac{V}{V_0}\right)$$

$$= A_e N_e e \sqrt{\frac{kT_e}{2\pi m_e}} \exp\left(\frac{V}{V_0}\right) \qquad (2)$$

where

A_e = area of the spherical collector

$$V_0 = kT_e/e \qquad (3)$$

To neutralize the negative surface charge, the plasma, in effect, surrounds the sphere with a positive ion sheath (a region where the ion-to-electron number density ratio is much greater than unity) which is the order of a few centimeters thick for a collector in the ionosphere between altitudes of 100 and 400 km. The sheath increases the effective area of the sphere for ion current by a factor $(a/r)^2$, where a is the sheath radius and r is the sphere radius; thus the ion current is given by

$$I_p = AJ_p(a/r)^2 = AN_p e \sqrt{\frac{kT_p}{2\pi m_p}} (a/r)^2 \qquad (4)$$

The net current to the sphere I is the sum of the electron current (2) and the ion current (4), assuming $N_p = N_e$; thus

$$I = I_p + I_e = ANe\left[(a/r)^2 \sqrt{\frac{kT_p}{2\pi m_p}} - \sqrt{\frac{kT_e}{2\pi m_e}} \exp(V/V_0)\right] \qquad (5)$$

The volt-ampere characteristic of the sphere, calculated from (5), is shown by the solid curve of Figure 2. The AB portion (ion saturation region) is due almost entirely to ions, as all 'thermal' electrons are repelled by the negative sphere. From about the point B to the plasma potential, the electron current, as indicated by I_e on the figure, becomes increasingly predominant.

Consider a second identical sphere to be some distance from the first sphere, with a variable voltage δV connected between the spheres. The volt-ampere characteristic of the second sphere can be represented by the dashed line in Figure 2. This curve is shown inverted with respect to that of the first sphere, for a voltage applied between the spheres forces the potential of one of them positive (net electron current flow) and the other negative (net positive ion current

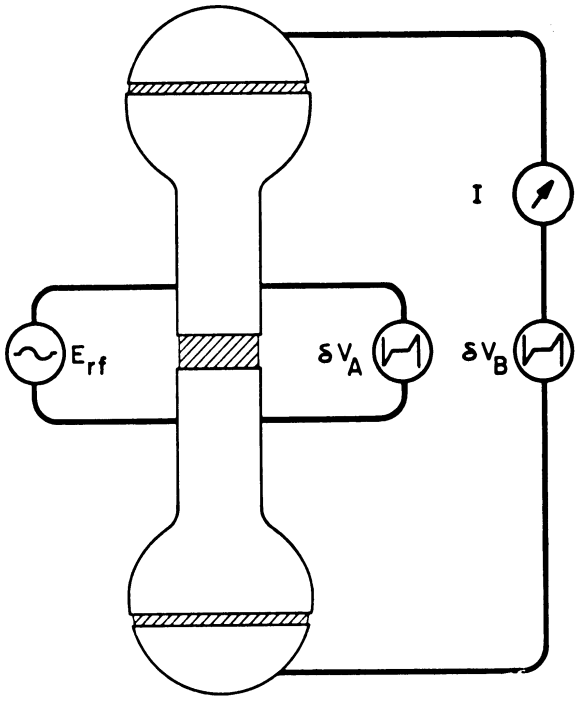

Fig. 4. A schematic representation of the dumbbell probe.

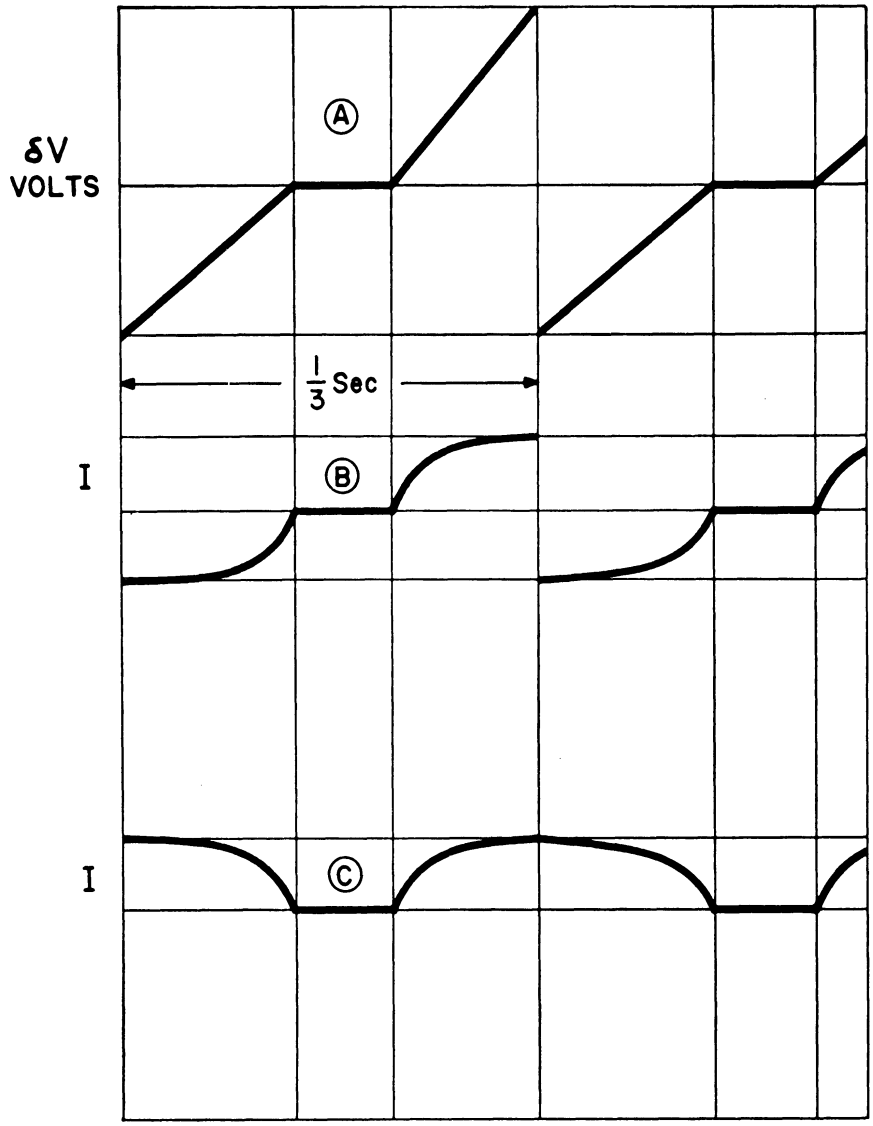

Fig. 5. Typical voltage-current curves for the dumbbell probe: (*a*) applied voltage; (*b*) resulting current; (*c*) current as it is expected to appear on telemetry.

flow). The sphere potentials, V_1 and V_2, adjust continuously to meet the zero net current requirement of the whole probe system over the entire range of the applied δV.

The volt-ampere characteristic of the symmetrical pair of spheres is obtained graphically from Figure 2 by plotting the net current I for a suitable range of δV as shown in Figure 3. Thus, the vertical displacement of this composite curve represents the current that would be observed to flow between the two spheres if connected by a generator of voltage δV. As in Figure 2, the outer, linear portions represent ion saturation current to the more negative sphere.

A practical probe. A physically realizable probe that is a very good approximation of the above idealized sphere-pair can be achieved. Figure 4 illustrates schematically its essential features. The two outer hemispherical portions are insulated from the adjacent funnel-shaped electrodes and are interconnected by a suitable sawtooth generator and series connected 'ammeter' (solid-state current detector). The applied voltage δV_s and the resulting current I comprise the desired 'raw data' from which electron temperature and positive ion density are computed.

The funnels, insulated from each other as well as from the hemispheres, are connected by a generator δV_4 producing a voltage identical in

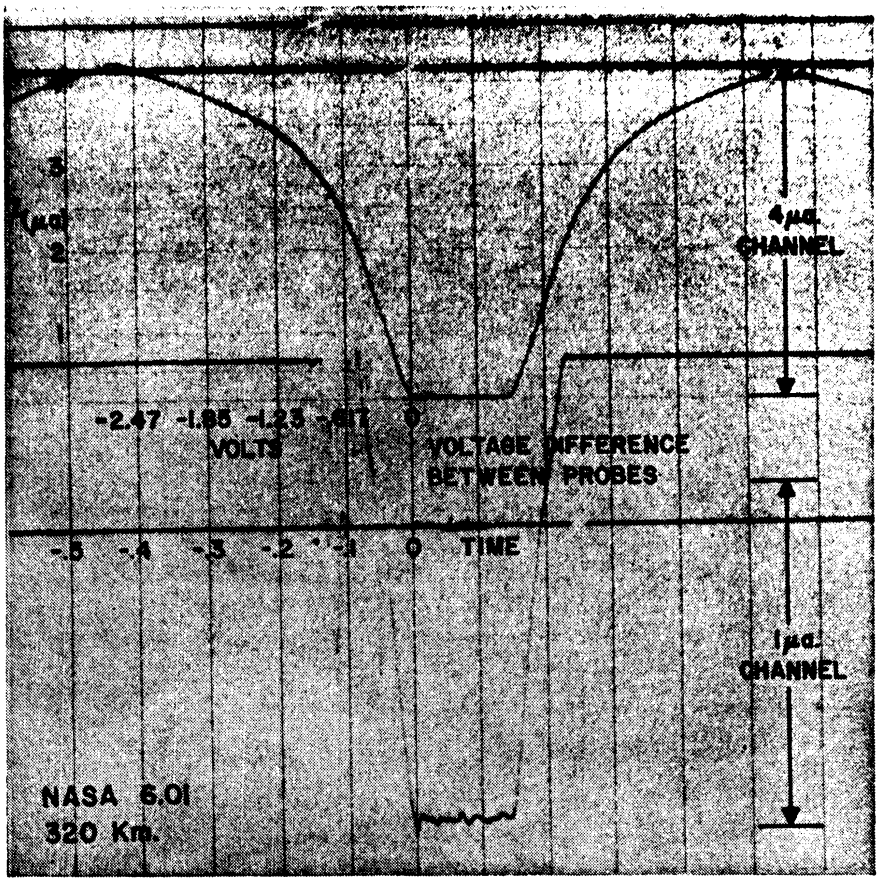

Fig. 6. A telemeter record showing the volt-ampere curve of the dumbbell probe.

magnitude and phase to δV_s. The funnels thus serve as guard electrodes for the hemispheres, resulting in a system that very closely approximates the system of two isolated spheres discussed above. The like generators and essentially identical areas of the hemispheres and funnels assure that there will be no significant potential difference between each hemisphere and its associated guard-funnel. Thus, a series of spherical equipotential surfaces can be considered to exist about each hemispherical electrode.

The indicated voltage source E_{RF} (Figure 4) represents the telemetry source which employs the dumbbell as a nearly ideal dipole antenna. The telemetry frequency employed is sufficiently high (approximately 240 Mc/s) so that the d-c probe system and RF telemetry system can act independently. The fact that the local charged particles are unaffected by the RF field will be discussed later.

The dumbbell probe is ejected from the launching rocket's nose-cone at about 80 km, to effect the desired isolation in the ionosphere. The rocket orientation at ejection, the ejection technique (forward by spring action from a 'clamshell' nose-cone) and the moment of inertia ratio for the dumbbell generally result in an end-over-end motion (typically 4-second period) in a near vertical plane. Additional equipment sometimes carried by the rocket, but not ejected, includes a radio Doppler system (DOVAP) employed for precision trajectory determination. On some occasions, as will be discussed, a 'two-frequency beacon' is carried on the rocket to provide additional and comparative data. It is not separated from the rocket.

Electrical characteristics. To detect sheath distortion and possible photo-electric current effects (to be discussed later) a two-section sawtooth voltage waveform as depicted in Figure 5*A* was selected. The magnitude was chosen on the basis of the anticipated electron energies, and the slope and repetition rate by measurement localization needs, the quantity of data desired, and the frequency response of the current detector and telemetry system. Figure 5*B*

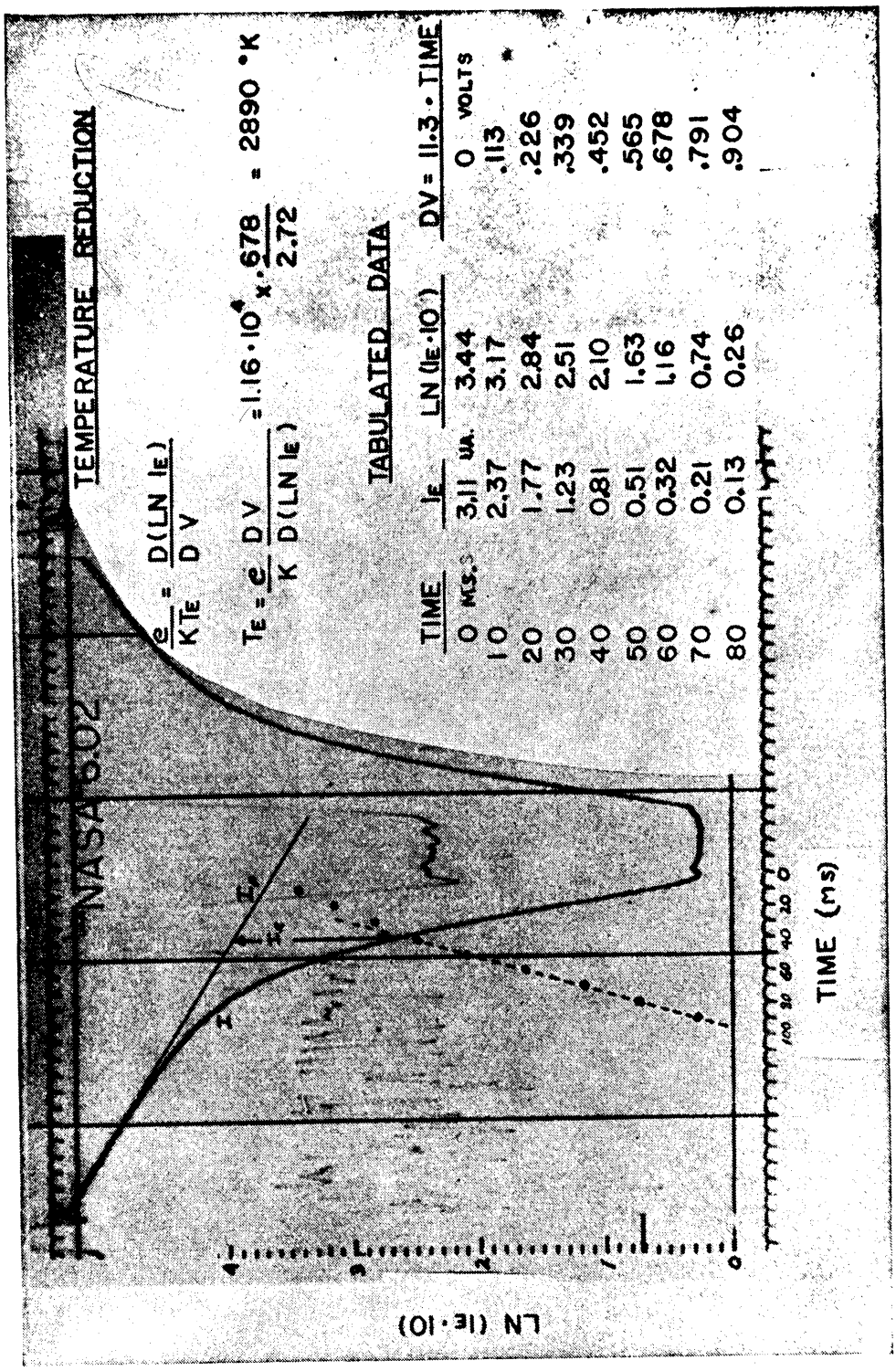

Fig. 7. An illustration of the technique of electron temperature data reduction.

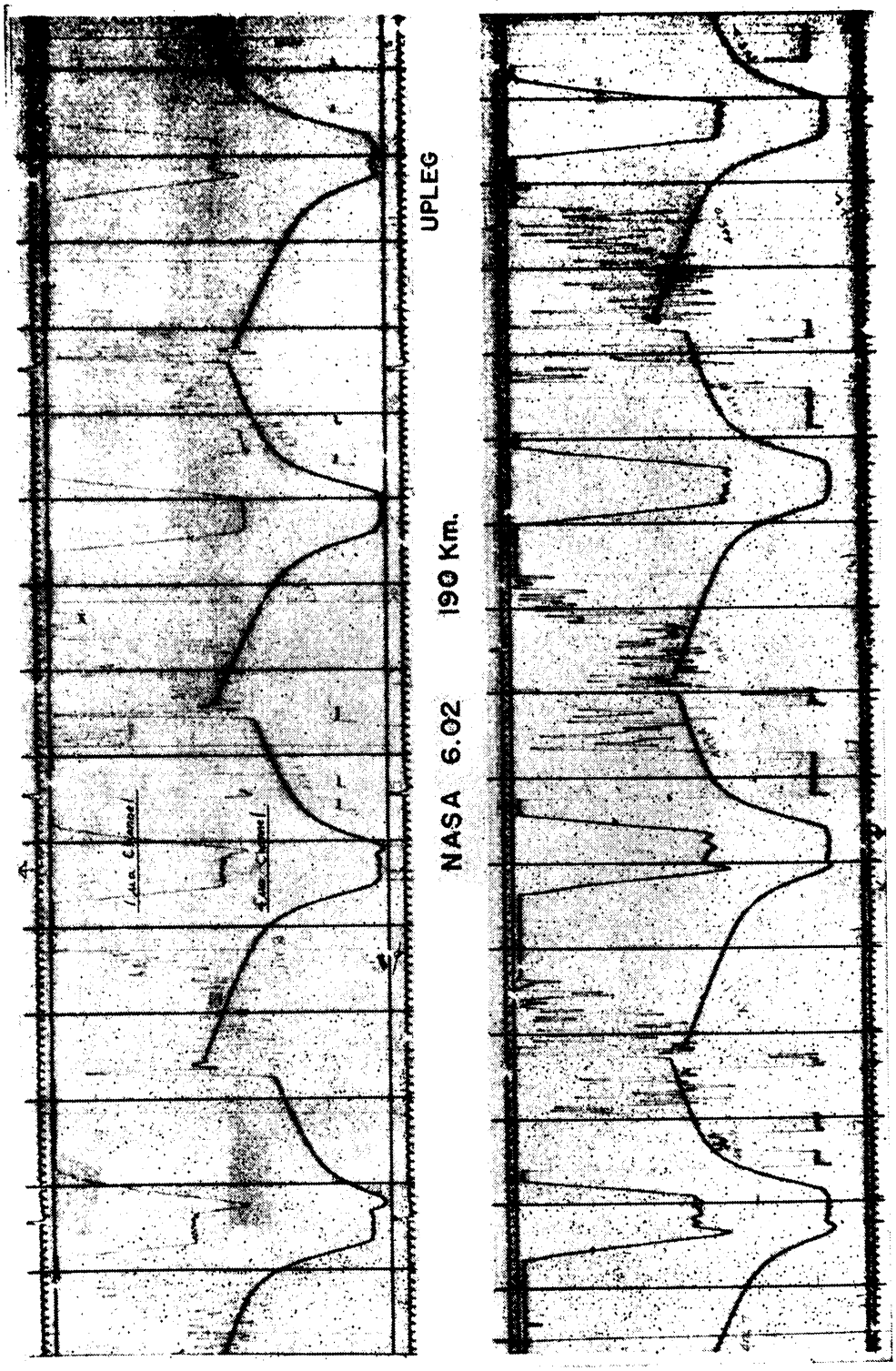

Fig. 8. Photographs of telemetry records showing the effect of probe velocity on the dumbbell volt-ampere characteristics.

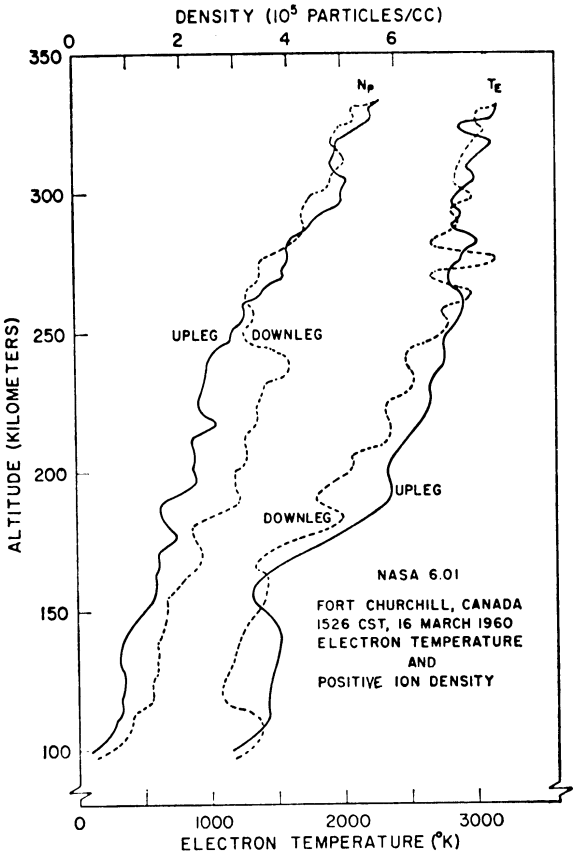

Fig. 9. Electron temperature and ion density for NASA 6.01.

illustrates a typical predicted current characteristic, and Figure 5*C* shows the expected current as it would appear on the telemetry record, the negative-going portion reversed in position because the ring-modulator current detector employed is magnitude sensitive only. Figure 6 is a portion of a flight telemetry record shown to permit comparison of the predicted and observed characteristics. The upper trace, as labeled, is the output indication of a current detector having about 4-microampere full-scale sensitivity. The lower trace results from a series-connected, 1-microampere detector which is quickly saturated by the currents encountered in the *F* region but which serves well for *E*-region measurements. The ion-saturated regions of the characteristic noted in the discussion relative to Figures 2 and 3 are clearly evident in the flight record.

Data reduction. The analysis of the data provided by curves such as shown in Figure 6 is straightforward, and the theoretical basis for the analysis is illustrated by the following.

1. The electron temperature determination: Figure 7 illustrates the manner in which the electron current vs. δV is derived from a dumbbell volt-ampere characteristic. From graphs such as shown in Figure 7, the electron current-vs.-probe voltage V is obtained. Referring to equation 2 and taking the logarithm

$$\ln I_e = \ln [AN_e e\sqrt{kT_e/2\pi m_e}] - V/V_0 \quad (6)$$

one obtains a linear equation in V (probe voltage) and $\ln I_e$ (electron current) whose slope is $V_0 = e/kT_e$. Since k and e are known constants, T_e can be determined. Hence, each volt-ampere characteristic measured may be interpreted in terms of the electron temperature of the plasma.

2. The ion density determination: Since the ion-saturated region of the curve is due solely to the collection of ions, current measured in this region at particular voltages is a measure of the ion flux at the sheath edge (essentially the undisturbed plasma). Thus, using the known potential V, one computes the sheath effect term, $(a/r)^2$, the current density at the sheath

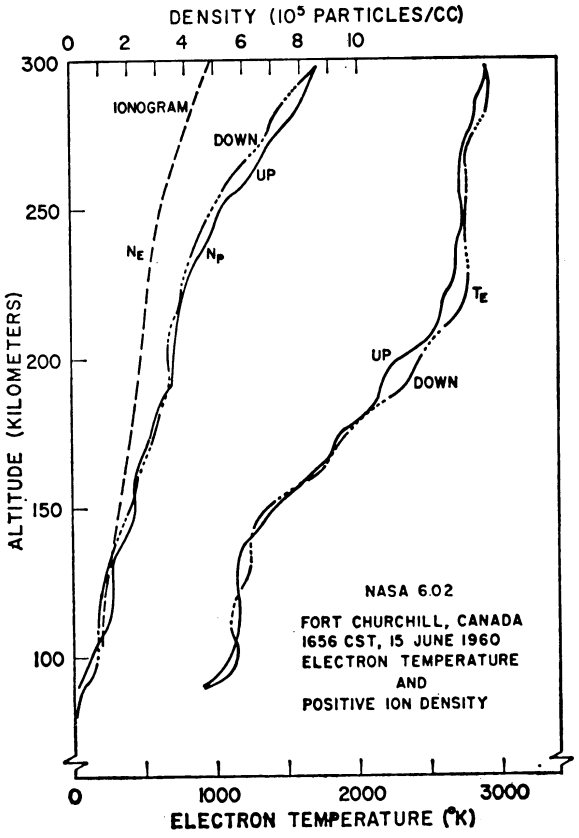

Fig. 10. Electron temperature and ion density for NASA 6.02.

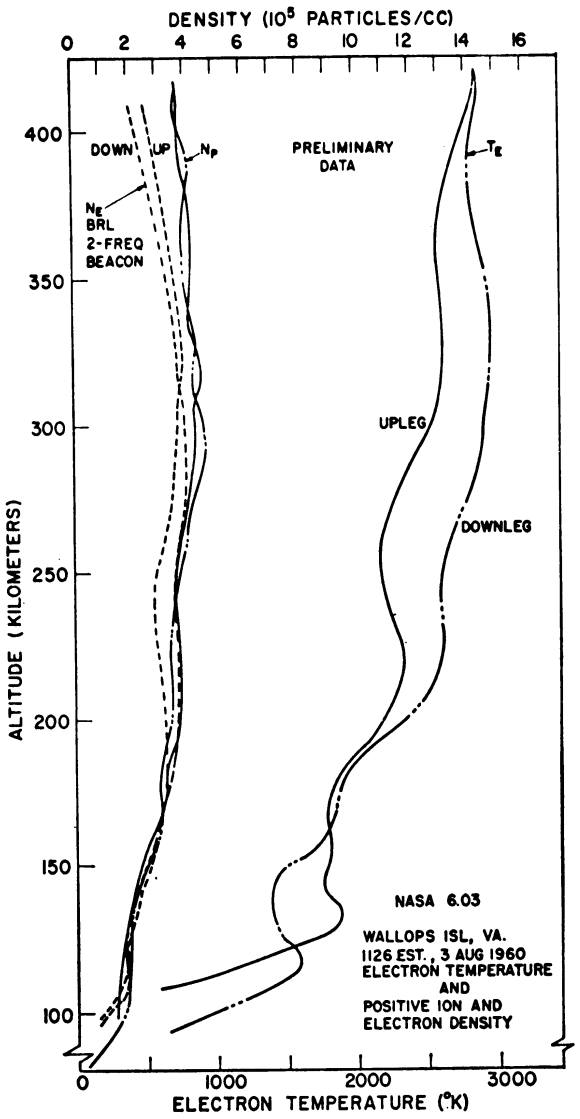

Fig. 11. Electron temperature, ion density, and electron density data for NASA 6.03.

edge, J_p, and hence the ambient ion density N_p. Reference to equation 4 shows that the N_p reduction requires that the ion temperature be measured or assumed. Since the data presented below indicate nonthermal equilibrium at these altitudes, it is not entirely valid to use the measured electron temperature in the density calculation. However, since T_e is the only *measured* temperature available in these data, the authors have elected to use it and make corrections later when the temperature relations are better understood. The error that results is not extremely serious, however, since T_p enters as the square root.

The above discussion indicates the major steps in the reduction of dumbbell probe data for the simplest case as illustrated in Figure 7, which shows a volt-ampere curve recorded near the peak of the trajectory of the flight noted.

At altitudes 50 to 100 km below the apogee, the rocket velocity becomes appreciable in comparison with the average ion velocity. The result is an increasing distortion of the sheath and of the ion current characteristic of a sphere. The current becomes dependent in part upon the angular orientation of the probe with respect to the velocity vector. Figure 8 is a photograph of two portions of the telemetry record of a flight in a region where the probe velocity is significantly higher than the ion velocity. These curves should be compared with Figure 6 which shows an apogee case where only the horizontal component of the velocity remains. It should be noted that these distortions in the current characteristic are due only to distortion of the ion component of the current so that the electron

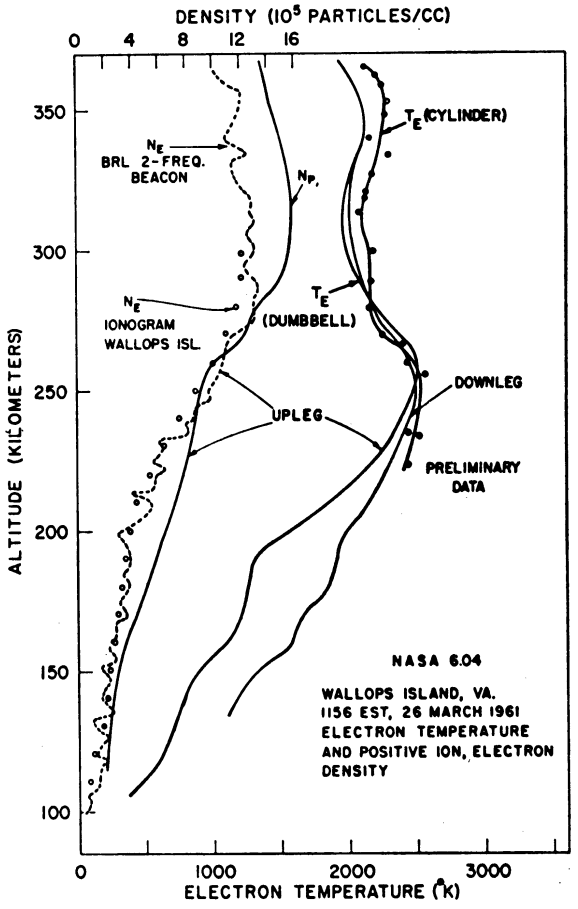

Fig. 12. Electron temperature, ion density, and electron density for NASA 6.04.

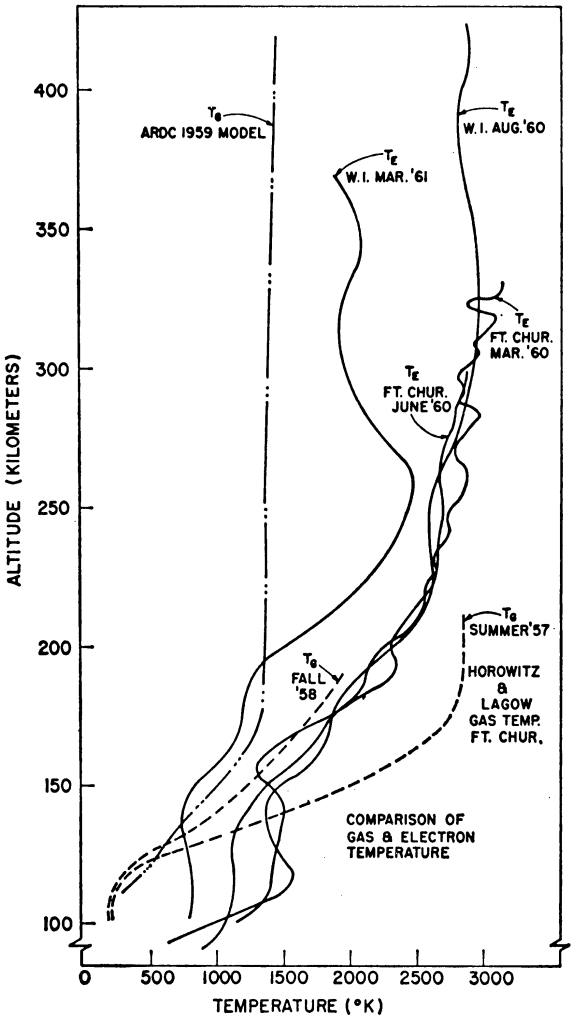

Fig. 13. Summary of electron temperature data.

current, obtained in the same manner as shown in Figure 7, as explained earlier, may still be used to obtain electron temperature. On the other hand, ion density data reduction must consider the effects of velocity.

Recently reported studies of volt-ampere relationships that take into account a superimposed directed ion velocity [*Hoegy and Brace*, 1961], and extensive analysis of the data obtained have shown, as noted above, that the electron temperature data reduction can be made without introducing significant error even though there is an appreciable velocity component. A demonstration of the validity of this statement is not appropriate to this paper and the reader is referred to the report noted. It should be observed, in addition, that although the ion velocity and rocket velocity are of the same order in vertical sounding flights to several hundred kilometers, the rocket velocity is always negligibly small in comparison with electron velocity.

Ionosphere parameters measured by the 'dumbbell' technique. The electron temperature and ion density data obtained from four dumbbell flights are shown in Figures 9, 10, 11, 12, and 13. All four flights took place during the daytime, under varying ionosphere conditions, at somewhat different times of the year, and at two different latitudes: in the auroral zone at Fort Churchill, Manitoba, Canada, (59°N) and at Wallops Island, Virginia (38°N). The statistics of the flights are summarized in Table 1, and 10-km interval data are tabulated in Tables 2 and 3.

Each profile represents a series of data points, each point being obtained from a running average of many individual measurements. Figure 14 illustrates a typical averaging situation. Many volt-ampere curves (1–3000) are obtained for each rocket flight during ascent and descent, and each curve yields an electron temperature. The expanded sections of the curve of Figure 14 show the individual electron temperature data points obtained during two typical 10-km altitude slices. It should be noted for a typical case that the 12 consecutive temperatures are measured in approximately 2 seconds so that each *mean* temperature represents an average over 2 seconds of flight, but each individual point a very small altitude interval.

Figure 11 also shows curves of electron density obtained through use of a two-frequency beacon[3] on the same rocket from which the dumbbell was ejected. Similar data obtained from flight NASA 6.04 are shown for comparison in Figure 12. Additional data resulting from simultaneously obtained ionograms are also presented for comparison.

Several conclusions seem apparent upon inspection of the data:

(*a*) The electron temperatures are significantly greater than generally accepted neutral particle temperatures, particularly for disturbed ionosphere conditions (NASA 6.01, 6.02, 6.03), where a factor of 2 is generally apparent in the temperatures. The authors have chosen to in-

[3] Equipment supplied and operated, and data reduced and provided, through courtesy of W. W. Berning, Aberdeen Proving Ground, Aberdeen, Maryland.

TABLE 1. Dumbbell Probe Rocket Statistics

Rocket Serial No.	Date	Time	Location	Ionospheric Condition	Rocket
NASA 6.01	3/16/60	1526 CST	Ft. Churchill	Aur. Zone, spread *F*	Aerobee 300
NASA 6.02	6/15/60	1656 CST	Ft. Churchill	Aur. Zone, near quiet	Aerobee 300
NASA 6.03	8/ 3/60	1126 EST	Wallops Is.	Magnetic storm end	Aerobee 300
NASA 6.04	3/26/61	1156 EST	Wallops Is.	Quiet	Aerobee 300

TABLE 2. Tabulated Dumbbell Probe Data

	NASA 6.01		NASA 6.02		NASA 6.03		NASA 6.04	
Alt., km	Upleg, T_e(°K)	Downleg, T_e(°K)	Upleg, T_e(°K)	Downleg, T_e(°K)	Upleg, T_e(°K)	Downleg, T_e(°K)	Upleg, T_e(°K)	Downleg, T_e(°K)
80								
90			900	900				
100	1160	1270	1100	1140		970		
110	1430	1360	1150	1100	750	1460	400	
120	1410	1070	1155	1140	1390	1570	600	
130	1490	1140	1150	1235	1870	1430	700	
140	1520	1240	1245	1245	1750	1395	780	1170
150	1410	1370	1410	1360	1770	1515	880	1330
160	1370	1440	1650	1670	1800	1780	1090	1580
170	1700	1440	1820	1840	1795	1850	1200	1660
180	2040	1920	2010	2040	1875	1930	1250	1850
190	2350	1810	2160	2300	2040	2120	1310	1910
200	2330	2050	2300	2425	2200	2370	1570	1990
210	2450	2340	2530	2600	2300	2545	1870	2150
220	2625	2330	2600	2745	2335	2620	2090	2260
230	2650	2530	2675	2765	2295	2630	2270	2300
240	2780	2470	2700	2745	2210	2620	2390	2440
250	2800	2780	2730	2755	2185	2625	2470	2500
260	2900	2880	2710	2760	2200	2690	2510	2350
270	2830	2640	2740	2765	2260	2775	2375	2210
280	2970	2720	2815	2880	2365	2860	2200	2180
290	2900	2880	2870	2920	2460	2910	2080	2100
300	2880	2960			2560	2935	1990	2040
310	2970	2900			2615	2960	1960	2010
320	3000	3040			2625	2980	1975	2020
330	3165	3010			2625	2980	2040	2050
340					2630	2975	2120	2120
350					2615	2955	2120	2120
360					2595	2925	2030	2030
370					2615	2880		
380					2660	2845		
390					2715	2825		
400					2790	2870		
410					2860	2910		
420					2875	2920		

clude the 1959 ARDC temperature curve (see Fig. 13) for comparison as it has become a familiar reference curve. This curve is not believed to be seriously in error, being possibly somewhat low, for daytime conditions in the region shown. The general accuracy is borne out by an increasing amount of published and unpublished data obtained from satellite drag, sodium releases, and ion density profiles that show somewhat higher temperatures. The direct measurement data of Horowitz and LaGow are also included for comparison. These apparently high gas temperatures are not explained except to note that their data result from measurements made at the time of a solar cycle maximum, at high latitude.

(*b*) There is a significant difference between electron temperatures for a quiet and for a disturbed ionosphere. Also, there appear to be greater secondary (fine structure) variations at Fort Churchill under spread *F* as compared with quiet conditions.

(*c*) There are clear differences between ascent and descent values of Figure 12 data, particularly in the F_1 region. It should be noted, however, that there exist both time and spatial differences between ascent and descent paths,

TABLE 3. Tabulated Dumbbell Probe Data

Alt., km	NASA 6.01		NASA 6.02		NASA 6.03		NASA 6.04	
	Upleg, $N_p \times 10^5$	Downleg, $N_p \times 10^5$	Upleg, $N_p \times 10^5$	Downleg, $N_p \times 10^5$	Upleg, $N_p \times 10^5$	Downleg, $N_p \times 10^5$	Upleg, $N_p \times 10^5$	Downleg, $N_p \times 10^5$
80				0				
90			0.15	0.34		1.00		
100		0.60	0.61	0.80	1.40	1.60		
110	.71	1.02	1.15	0.85	1.48	1.80		
120	.83	1.43	1.40	1.00	1.56	1.71	2.10	
130	.72	1.55	1.37	1.23	1.70	1.90	2.30	
140	.86	1.58	1.84	1.60	1.95	2.18	2.55	
150	1.28	1.68	2.20	2.00	2.30	2.45	2.90	
160	1.48	1.94	2.20	2.30	2.70	2.90	3.40	
170	1.47	2.38	2.58	2.70	3.10	3.00	4.35	
180	1.75	2.15	2.90	3.01	3.20	3.00	5.00	
190	1.70	3.02	3.41	3.40	3.50	3.17	5.60	
200	2.20	2.90	3.56	3.40	3.70	3.40	6.40	
210	2.15	3.23	3.64	3.42	3.80	3.47	7.20	
220	2.45	3.54	3.81	3.81	3.75	3.40	7.80	
230	2.40	3.53	4.17	4.00	3.70	3.50	8.30	
240	2.50	4.00	4.80	4.39	3.60	3.60	8.65	
250	2.90	3.15	5.23	5.00	3.65	3.80	9.10	
260	3.25	3.32	6.20	5.57	3.83	4.00	10.10	
270	3.95	3.45	6.82	6.50	4.02	4.22	12.30	
280	3.97	3.95	7.66	7.08	4.20	4.50	13.20	
290	4.45	4.23	8.30	7.85	4.39	4.73	15.00	
300	5.00	4.75			4.40	4.68	15.60	
310	4.80	5.10			4.50	4.40	15.80	
320	5.00	4.87			4.59	4.40	15.80	
330	5.50	5.20			4.30	4.40	15.60	
340					4.20	4.13	15.00	
350					4.20	4.00	14.40	
360					4.25	3.95	13.80	
370					4.20	3.98		
380					4.05	4.10		
390					3.90	4.18		
400					3.80	3.84		
410					3.84	3.72		

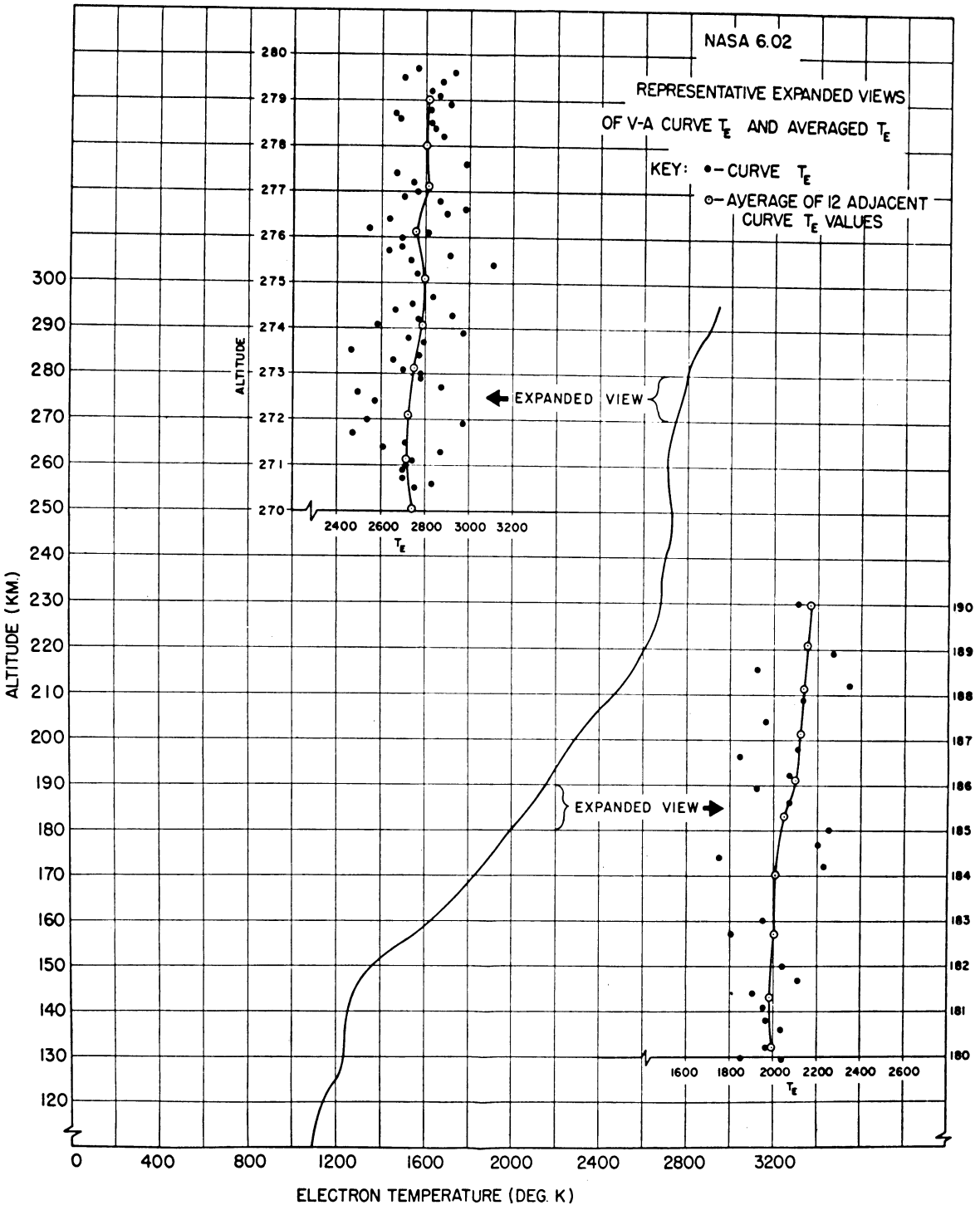

Fig. 14. An expanded curve for NASA 6.02.

typically 8 minutes and 200 km horizontal separation for the *E*-region data.

(*d*) There is good agreement between electron density data (as derived from both beacon and ionosonde equipment) and ion density data (Fig. 12) for Wallops Island but not as good for the single case at Fort Churchill for which comparative data were available.

(*e*) A distinct temperature inversion is apparent above 250 km in the Wallops Island data; see Figures 12 and 13.

Discussion. The fact that the quiet iono-

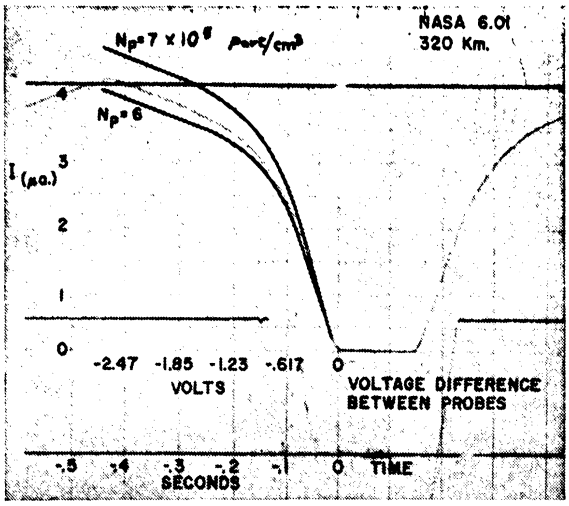

Fig. 15. A comparison of the predicted and observed volt-ampere characteristic.

sphere electron temperatures, and particularly the disturbed ionosphere electron temperatures, are clearly greater than generally accepted neutral particle temperatures (Fig. 13) seems to the authors to demonstrate that thermal equilibrium does not exist, at least in this region. The curve determined for quiet conditions has a negative gradient at the highest altitude attained, thus suggesting that the neutral particle temperature is being approached above 350 km. On the other hand, those temperatures observed under disturbed conditions show no tendency to approach the expected isothermal temperature of the neutral particles and, presumably, of the ions. Thus, to the authors, these data suggest that possibly one should not expect equilibrium at even higher altitudes.

Since these data are not in agreement with other recently published data, and the conclusion reached is not in accord with generally held concepts relative to atmospheric thermal equilibrium at 350 km and higher altitudes [e.g., *Jackson and Bauer,* 1961], the authors have believed it particularly important to establish the validity of the technique and the data presented, and, therefore, have given considerable thought and effort to checking the work and providing other means of establishing confidence in the results. Figure 15 illustrates one approach taken in this regard.

As noted previously, the theoretical aspects of the dumbbell technique have been studied extensively, and the general experimental results have been found to be in very good agreement with predictions. To provide a consistency check of the technique, a typical volt-ampere curve as observed in flight was reduced to electron temperature and ion density. These data were then used to compute the volt-ampere curve that a dumbbell should exhibit under the observed conditions. Figure 15 shows the results of the computations drawn on a photograph of the portion of the telemetry record from which the data were deduced. The computed volt-ampere curves shown correspond to two values of ion density: $N_p = 7 \times 10^5$ ions/cc, and $N_p = 6 \times 10^5$ ions/cc, the latter value being the density originally deduced from the record. The value of N_p that satisfies the experimental curve is 6.4×10^5 ions/cc, indicating that, in this instance (chosen at random), the observed N_p was less than 10 per cent high. This is known to be due to the effect of probe motion which increases the ion current and was not considered in the N_p reduction. The consistency demonstrated between experimental and theoretical curves appears to the authors to substantiate the general validity of the theoretical approach and the experimental technique.

A second, essentially unrelated consideration, concerns the electrons sampled by the dumbbell

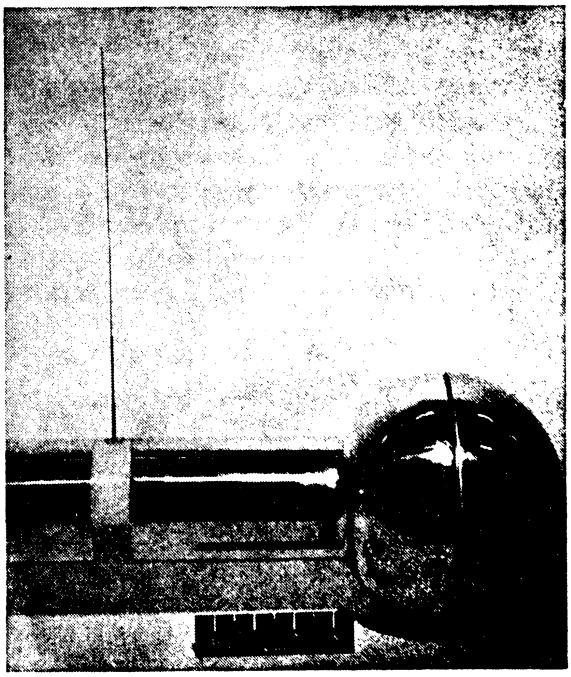

Fig. 16. A photograph of the NASA 6.04 dumbbell showing also the small cylindrical probe.

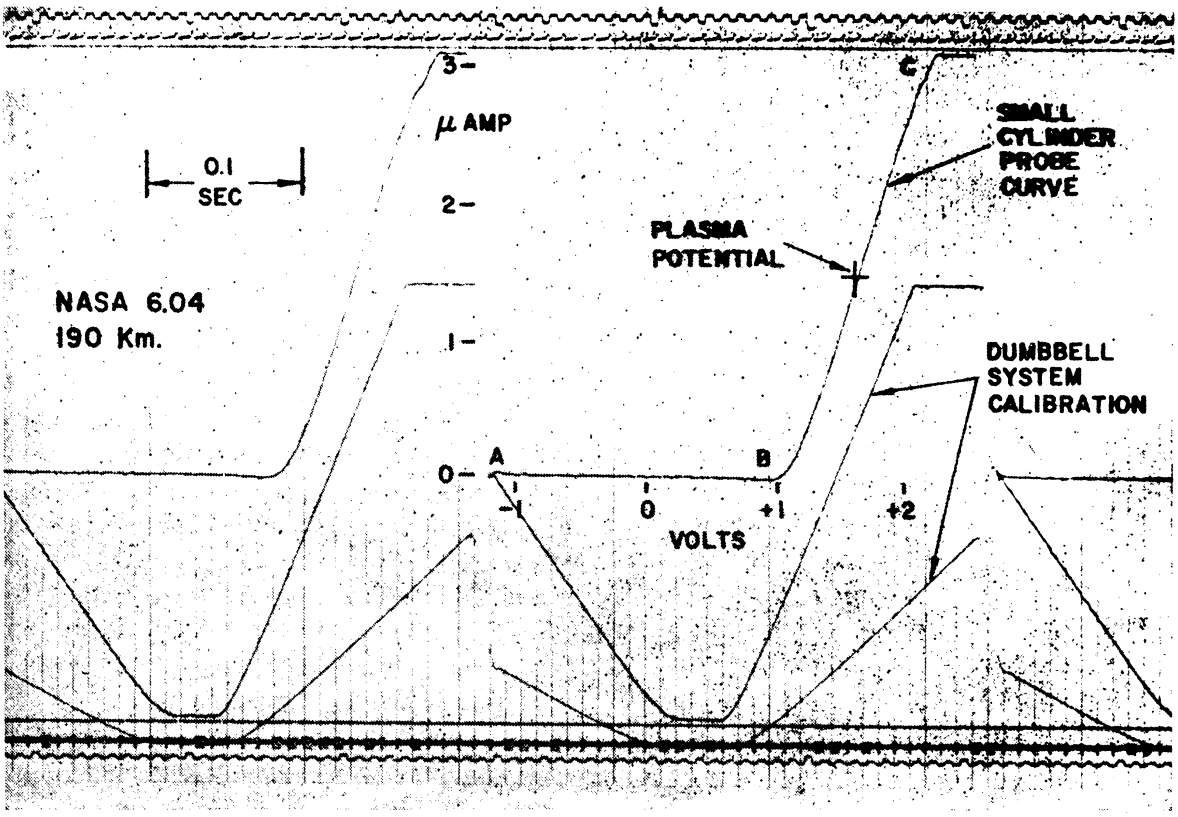

Fig. 17. A photograph of a portion of the telemetry record from NASA 6.04, showing the signal from the small cylindrical probe.

probe and their relation to the entire population of thermal electrons. Figures 2 and 3 show the individual volt-ampere curves of the hemispheres before and after consolidation. Figure 2 is particularly useful in understanding how an applied potential δV divides between the hemispheres. δV causes the hemispheres to assume potentials V_1 and V_2, respectively, and results in a net current, I_a. It is clear that the negative-going hemisphere 'accepts' most of the applied potential, i.e., $(V_1 - V_w) > (V_w - V_2)$ where $\delta V = V_1 - V_2$. The effect of this δV division is that neither probe potential can rise much above V_w so that only those electrons having energies exceeding V_w are sampled. The question thus naturally arises whether the temperature as indicated by these electrons is equivalent to the temperature that would result from sampling the entire population.

To verify the assumption, and the authors' belief, that the measured electrons are representative of the whole population, an independent probe experiment was carried out using a small cylinder as one electrode and the whole dumbbell as a second electrode, to provide a probe system with a large area ratio. Thus, in this case, the entire dumbbell was employed as the reference electrode with a typical sawtooth voltage applied between it and the small cylindrical electrode. The configuration is illustrated in Figure 16, which shows a portion of the dumbbell used for flight NASA 6.04. The three parts of the cylindrical probe are: a spring, a short guard cylinder and a long collector cylinder.

Figure 17 shows some of the telemetry record for this cylindrical probe (volt-ampere curves), during one of the many 4-second intervals when the cylindrical probe was in use and the dumbbell circuits were being calibrated (dumbbell measurements were made during alternate 4-second periods). The volt-ampere characteristic of the cylindrical probe (see Fig. 17) shows a ratio of electron current (B-C portion) to the ion current (A-B portion) which is much greater than the same ratio for the dumbbell probe (see

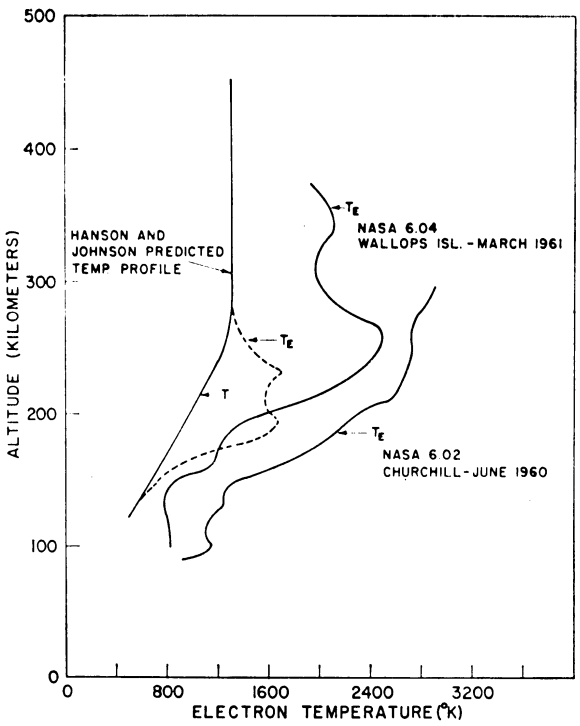

Fig. 18. Theoretical and experimental electron temperature data.

Fig. 6). This is a consequence of the small cylinder being driven far more positive than is possible for a dumbbell hemisphere. A preliminary data analysis has been accomplished and the electron temperature results of the small cylinder probe are plotted with the dumbbell temperatures on Figure 12. This analysis is to be considered preliminary since this was the first flight using the cylinder configuration; however, the authors have sufficient confidence in these data to conclude that the characteristic temperature of electrons as measured by the dumbbell is equivalent to that of the entire thermal electron population as measured by the cylinder.

Although both approaches employ the electrostatic probe technique it should be noted that the current 'collection' mechanism of the small cylinder probe is quite different from that of the dumbbell. In the dumbbell case the ion current is described as being 'sheath area limited,' and for the cylindrical probe, 'orbital limited.'

Concluding remarks. This paper has presented a brief review of a particular approach to making direct measurements of electron temperature and ion density in the earth's ionosphere. Although the basic technique is not of recent origin, the authors believe that the data represent new information, now readily obtainable because of advances in instrument technology. Moreover, the authors believe that the data presented make necessary a revision of the concept of thermal equilibrium in the daytime ionosphere between electrons and neutral particles, at least up to 420 km and particularly in a disturbed ionosphere. The variation of electron temperature observed shows good correlation with the state of the ionosphere, higher and more locally variable temperatures being observed for a more disturbed ionosphere. It is observed also that the Wallops Island data taken under quiet conditions show reasonably good agreement qualitatively with the theoretical data of *Hanson and Johnson* [1961], see Figure 18, which were computed for conditions corresponding, approximately, to a quiet ionosphere.

Theoretical studies leading to the temperature equilibrium concept generally lead one to conclude that the collision frequency between electrons and neutral particles and ions is sufficiently high throughout the ionosphere for the excess energy which an electron acquires in the ionization process to be very rapidly distributed among the other species. It is clear, however, that the process of energy transfer between the electrons, and between ions and/or neutral particles, must be much more efficient than that between electrons and ions or neutral particles. This is true because of the very large mass ratio in the latter event. Thus, one should expect the electrons to be in equilibrium among themselves and the ions and neutral particles to be in equilibrium with each other because of the low mass ratio.

The phenomenon of two kinds of particles existing in equilibrium at different temperatures is observed commonly in the laboratory for gases at relative high density, and hence at very high collision frequency, as compared with the ionosphere. Thus, by analogy, one should not expect to find complete thermal equilibrium in the ionosphere. It is required only that there be a source of energy that affects electrons selectively. Solar radiation does this, providing adequate energy to ionize a modest fraction of the *F*-region oxygen atoms and thus to raise electrons to many volts of energy.

It thus seems to the authors that the neutral particle and the electron temperatures should

be expected to be different in the daytime ionosphere and that the major question is one of the magnitude of the difference. The general factor-of-2 difference observed in the data corresponds to an electron energy excess of only about 0.15 ev, and since electrons resulting from He II ionization of oxygen initially have 28 ev of energy, the excess energy observed seems entirely credible. The authors thus conclude that the temperature results presented are reasonable and correctly represent the conditions which held at the time the measurements were made.

Accuracy. The temperature derived from each volt-ampere curve has a standard deviation of approximately 10 per cent of the mean. The profiles obtained through the averaging technique have an accuracy of somewhat better than 5 per cent above 130 km. Below this level, the error may be greater because the sheath conditions become more complex as the ion and electron mean free paths become comparable to the probe dimensions.

The general agreement observed between the electron densities as obtained by the two-frequency beacon system and the ionosondes, and the ion densities observed by the probe, is expected, since it would seem to be difficult to explain a *difference* except on a very local basis and under highly transient conditions because of the electric field implications of any predominance of charge of one sign over the other.

The much poorer agreement between electron density as determined from the ionosondes at Fort Churchill and the dumbbell ion densities taken simultaneously (Fig. 10) has not been explained. A similar departure observed at Wallops Island (Figs. 11, 12) above 300 km likewise has not been explained.[4] It should be noted, however, that the ion density result is based upon an assumption of *only* atomic oxygen ions at the 300- to 400-km level. If there were, for example, more hydrogen and/or helium ions than expected, the high current would be due to the higher ion mobility rather than a greater number of ions, and the computed density values would be too high. There is no experimental evidence at this time, however, to support such a hypothesis.

Further experiments are being prepared to provide additional data. For example, it is considered very important to conduct similar measurements in the nighttime ionosphere since equilibrium should be observed at that time. Thus, the next launching, planned for the fall of 1961, is scheduled for midnight. Both small cylinder and dumbbell measurements are contemplated for this and subsequent experiments. Additional experiments are underway that will permit simultaneous measurements of the temperature of both neutral particles and electrons to 250 km, and that will measure electron temperature for altitudes up to the order of 800 km.

Acknowledgments. The early flights mentioned in the paper, and on which the present series is based, were supported by the Geophysics Research Directorate of the Air Force, Cambridge Research Laboratories, and the Ballistic Research Laboratory of the Aberdeen Proving Ground. The work and flights reported herein were supported by the National Aeronautics and Space Administration.

We wish to acknowledge especially the contributions of John Maurer, Walter Hoegy, James Findlay, Hugh DiGiulio, and Lyle Slider, a few of the many individuals of the Space Physics Research Laboratory whose efforts in theoretical work, computer programming, data analysis, and equipment development and construction made possible the work reported. The contribution of launch support personnel at the Fort Churchill and Wallops Island sites is also gratefully acknowledged.

APPENDIX

Perturbations in the Measurements

1. *RF effects.* Two questions have been raised frequently in discussion of this work. The first question is concerned with the effect of the telemetry RF field on the local electrons. One can compute that, at the 230-Mc/s telemetry frequency, totally insignificant energy is imparted to electrons. To establish this experimentally, a dumbbell with a data storage system was flown during the equipment development stage. Electron temperatures measured in the complete absence of any field were judged to be within 5 per cent or better of the electron temperatures measured in the presence of the field. This figure is determined largely by the low resolution instrumentation in use at that time. In a more recent flight, NASA 6.04, the telemetry power

[4] A possible explanation is that initial velocities of ions at the sheath edge were not considered in the calculations. This effect [e.g., *Schulz and Brown*, 1960], although relatively small, would tend to reduce the indicated densities somewhat.

was periodically reduced by a factor of 5, but no differences were observed in the electron temperatures.

2. *Photoemission effects.* A second question frequently asked concerns the effect on the measurements of photoemission from the electrodes. The measurement of any current imbalance such as might be caused by photoemission is possible during the time when zero voltage is applied to electrodes (see Fig. 6). Typical values of current that have been measured are generally less than *Hinteregger's* [1959] values. The maximum photocurrent measured is less than 10^{-7} amperes and is insignificant in comparison with the normal ion and electron current encountered, which is usually about 4 to 6 microamperes at the F_2 maximum (see Fig. 15).

References

Berning, W. W., A sounding rocket measurement of electron density to 1500 km, *J. Geophys. Research, 65,* 2589–2594, 1960.

Boggess, R. L., L. H. Brace, and N. W. Spencer, Langmuir probe measurements in the ionosphere, *J. Geophys. Research, 64,* 1627, 1959.

Dow, W. G., and A. F. Reifman, Dynamic probe measurements in the ionosphere, *Phys. Rev., 76,* 987, 1949.

Hanson, W., and F. S. Johnson, Electron temperatures in the ionosphere, Tenth International Astrophysical Colloquium, Liege, Belgium, 1961.

Hinteregger, H. E., K. R. Damon, and L. A. Hall, Analysis of photoelectrons from solar extreme ultraviolet, *J. Geophys. Research, 64,* 961–969, 1959.

Hoegy, W., and L. H. Brace, *Scientific Rept. JS-1, University of Michigan ORA Rept. 03599-5-S,* June 1961.

Hok, G., N. W. Spencer, and W. G. Dow, Dynamic probe measurements in the ionosphere, *J. Geophys. Research, 58,* 235–242, 1953.

Hok, G., N. W. Spencer, W. G. Dow, and A. Reifman, Dynamic probe measurements in the ionosphere, *University of Michigan ERI Report,* August 1951.

Jackson, J. E., and J. A. Kane, Measurements of ionosphere electron densities using an RF probe technique, *J. Geophys. Research, 64,* 1074–1075, 1959.

Jackson, J., J. A. Kane, and J. C. Seddon, Ionosphere electron density measurements with the Navy Aerobee-Hi rocket, *J. Geophys. Research, 61,* 749–751, 1956.

Jackson, J. E., and S. J. Bauer, Rocket measurement of a daytime electron density profile up to 620 km, *J. Geophys. Research, 66,* 3055–3057, 1961.

Johnson, C. Y., E. B. Meadows, and J. C. Holmes, Ion composition of the arctic ionosphere, *J. Geophys. Research, 63,* 443–444, 1958.

Seddon, J. C., Propagation measurements in the ionosphere with the aid of rockets, *J. Geophys. Research, 58,* 323–335, 1953.

Schulz, G. J., and S. C. Brown, Microwave study of positive ion collection by probes, *Phys. Rev., 98,* June 1960.

(Manuscript received July 24, 1961; revised October 13, 1961.)